Hindawi
Journal of Sensors
Volume 2022, Article ID 9973299, 12 pages
https://doi.org/10.1155/2022/9973299

Research Article

Analysis on Influence Factors of Differential Pressure Detection of Gas Leakage

Yan Shi,[1] Jiaqi Chang,[1] Yixuan Wang,[2] and Liman Yang[1]

[1]*School of Automation Science and Electrical Engineering, Beihang University, China*
[2]*Engineering Training Center, Beihang University, China*

Correspondence should be addressed to Yixuan Wang; magic_wyx@163.com

Received 8 March 2022; Revised 24 August 2022; Accepted 7 September 2022; Published 10 October 2022

Academic Editor: Egidio De Benedetto

Pneumatic technology takes compressed gas as the power source, but the leakage of gas in the pipeline due to poor sealing or pipeline rupture affects the accuracy of pneumatic control, the flow of gas transmission, and even the emission of harmful gas. The air tightness of differential pressure method has broad significance in the study of tight leakage because of its simple operation, short detection time, and high precision. Bubbling method, acoustic emission detection method, and direct pressure detection method have the characteristics of difficult operation, environmental sensitivity and low detection accuracy. They are not suitable for effective and high-precision detection of leakage in harsh environment. The air tightness detection method of differential pressure method has the advantages of simple operation, short detection time, and high accuracy. It has extensive significance in the research of air tightness leakage. At present, the focus of differential pressure method is to keep the same charging state of the master tank and the tested tank. However, when the shape of the tested tank is irregular or difficult to copy, the influence of different master tank on differential pressure method leakage detection needs to be considered. In this study, a gas leakage flow calculation model is established. The influence of the inherent parameters of the master tank on the calculation of the pressure difference, temperature difference, and leakage between the two cavities is analyzed in the simulation. Finally, the master tank is set as a quasi-isothermal cavity, and the tested tank is set as 3 L and 5 L air tanks for leakage test. The maximum error of experiment of 3 L tank reaches 39 mL/min at the later stage of measurement, with a detection deviation of 14.4%. The maximum error of experiment of 5 L tank is 412.4 mL/min, with a deviation rate of 28.3%. This method can detect leakage with high precision in harsh environment.

1. Introduction

Pneumatic technology is a transmission technology with compressed gas as the power source. Pneumatic components and pneumatic systems are widely used in the mechanization and automation of factory production process because of their advantages of less pollution, low cost, strong anti-interference, and convenient maintenance. At present, in pharmaceutical, medical devices, electrical, automotive, and other industries, air tightness detectors are used to detect the air tightness of bottles, cans, and tubes. Air tightness detection is very important not only in pneumatic servo control system [1] but also in other pneumatic fields, such as pneumatic transmission [2–4], geological detection [5], pneumatic spring, and semiconductor manufacturing process [6], even the on-orbit operation of spacecraft is very important [7].

Common detection methods include bubbling method, acoustic emission detection method, and differential pressure detection method. Bubble detection method is a traditional air tightness detection method. The medium is mainly water and soap liquid. The tested tank is sealed and applied a certain pressure to its inner cavity and then immersed in the water tank to observe whether bubbles are generated and the position of bubbles, so as to judge whether the workpiece leaks and the leakage position. The detection

method has the advantages of simple operation and low cost. However, the efficiency of this method is low. At the same time, the tested workpiece must be dried and antirust treated after the test. The flow detection method refers to that when the workpiece has leakage, the gas filled in the closed chamber will overflow outward through the leakage so that the leakage of the measured workpiece can be detected quantitatively through the microflow tester. For the workpiece with small leakage, the flow detection method will take a long time. Therefore, this detection method is suitable for workpieces with large leakage. The direct pressure detection method refers to that the measured workpiece is filled with a certain pressure of gas. If there is leakage, the pressure in the cavity will drop after a certain time of reaction. The detection method has the advantages of simple operation, low cost, and fast detection, but limited by the accuracy of pressure sensor; it can only be applied to the field with low accuracy requirements [8, 9].

In the aspect of ultrasound testing method, Xiao et al. discussed the principle of ultrasonic wave generated by hole leakage and the relationship between sound pressure and hole size. A leak estimation method based on relation and the design of gas leak ultrasonic detection system are proposed [10]. Piazzetta et al. proposed to study the ultrasonic leakage detection technology [11]. Wang et al. proposed an ultrasonic leakage location method based on multialgorithm data fusion [12] and a cylindrical container gas leakage location method based on annular ultrasonic sensor array [13]. In addition, there is a negative pressure wave pipeline leakage detection method [14], or establish the functional relationship between the leakage and other influencing factors of the product, to judge the leakage [15]. In general, ultrasound testing method is difficult to be used in the running devices in practice. Similar to the ultrasonic method, it is used for gas detection in special occasions such as liquefied petroleum gas, which uses chemical methods to detect the concentration of a gas component in the environment to determine leakage [16]. However, this method is not universal, and the detection efficiency is generally low.

In terms of gas pipeline leakage, some scholars have proposed a new method combining optimization. Tan et al. proposed a new for fault diagnosis of gas leakage monitoring sensors based on Naive Bayesian classifier and probabilistic neural network [17]. Chi et al. proposed a new leak detection method based on improved adaptive filter. The parameters of this method are optimized by particle swarm optimization algorithm [18]. Jahanian et al. use extended Kalman filter to detect and locate leakage and use robust extended Kalman filter to compensate the influence of parameter uncertainty [19]. Doshmanziari et al. use the extended Kalman filter as the state observer to start leakage detection and use the sensor array to improve the system redundancy and leakage estimation accuracy [20]. But this method has a large amount of calculation and a slow detection speed. And the method needs to ensure that the gas is inside the long pipe, which the application conditions are limited.

The differential pressure detection method is similar to the direct pressure detection method. The differential pressure detection method also needs to prefill the tested workpiece with gas of a certain pressure, but this method needs a master workpiece as the comparison object. When the tested workpiece has leakage, the pressure difference between the two is detected by the pressure difference sensor, and the leakage is calculated according to this. When the structure of the selected master workpiece is completely consistent with that of the measured workpiece, all error factors existing in the detection process can be approximately ignored, and the accuracy of the differential pressure sensor is high, so the differential pressure detection method can accurately detect the workpiece with small leakage. The research on differential pressure method is relatively few, and the research carried out is to use the same master gas tank for the tested tank, such as Zhao et al. [21] studied the differential pressure method. However, this method does not consider the difference caused by the different temperature changes of the two gas tanks. This method is difficult to popularize because it is difficult to ensure the consistency of the two gas tanks. When the measured gas tank is irregular in shape or too large in volume to process, it is necessary to study the leakage differential pressure detection of asymmetric cylinder.

In order to solve the problems existing in the above leakage detection methods, the improvement of differential pressure detection method is carried out, and the air tightness of differential pressure method based on isothermal chamber is studied in this paper. Through simulation, the effects of different temperature parameters or volumes in the measurement stage and whether to use quasi-isothermal cavity on the measurement results of differential pressure method are analyzed. The effect of differential pressure method and the influence of different volume and leakage on the results are verified, as well as the measurement of air tightness through quasi-isothermal cavity by experiments.

2. Methods

2.1. Introduction of Differential Pressure Method. The principle of differential pressure air tightness detection is based on the ideal gas state equation, and the gas leakage rate is calculated by detecting the pressure change in the container. After a certain volume of container leaks a certain amount of gas, the pressure inside the container will have a pressure drop relative to the previous one. Therefore, the actual leakage rate of gas inside the container can be calculated by measuring the pressure drop inside the inner container for a certain time. The differential pressure leak detection experiment can be completed by the structure in Figure 1.

The flow of differential pressure detection method is as follows: charging-balance-measurement. The on-off valve action and energy exchange state in each stage will be analyzed in detail below.

(1) Charging stage

In this stage, the two inlet valves are opened at the same time, and the air source will charge the master chamber and the tested chamber at the same time until the set pressure is reached. At this stage, there is mass exchange between the

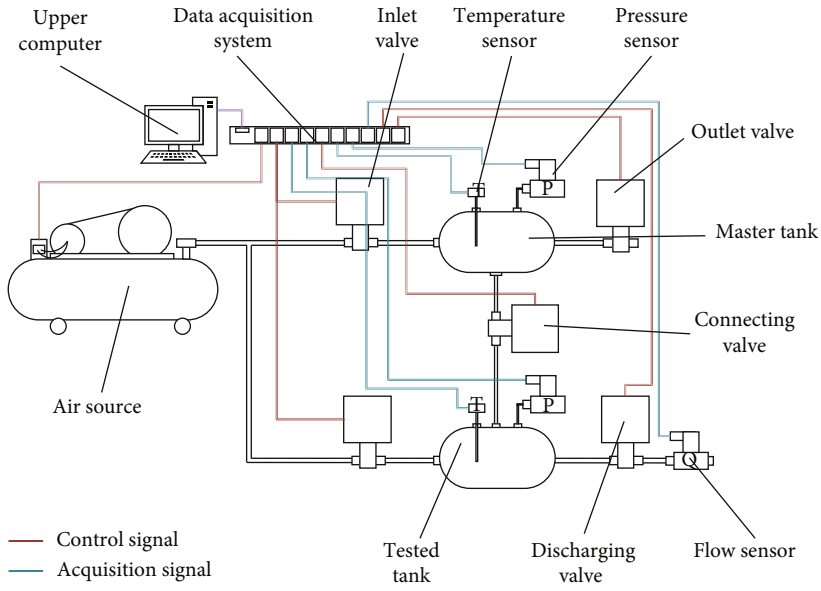

Figure 1: Differential pressure detection diagram.

master chamber and the air source and heat exchange with the external environment. There is also mass exchange between the tested chamber and the air source, mass exchange caused by leakage with the external environment, and heat exchange with the external environment.

(2) Balance stage

In this stage, the inlet valves of the two chambers are closed to interrupt the charging process, then the connection between the master chamber and tested chamber is opened to connect for a period to eliminate the temperature difference and differential pressure imbalance between the two chambers caused by inflation until the temperature of the two chambers returns to normal temperature.

(3) Measurement stage

When the temperature of the master chamber and the tested chamber have recovered to the ambient temperature, the connecting valve is closed to isolate the two chambers to start detection and judge whether the chamber is leaking through the signal of the differential pressure gauge. At this stage, the theoretical situation only exists when there is no heat exchange between the two cavities and the environment. However, in actual measurement, there is often a temperature difference between the two cavities and the environment in the detection stage due to insufficient balance time. In this case, the influence of corresponding heat exchange needs to be considered.

2.2. Charging Process Modeling. In the inflation stage, for the master cavity, it is obtained from the law of energy conservation.

$$\frac{d(C_v m T_{\mathrm{m}})}{dt} = C_p T_{\mathrm{s}} \frac{dM_{\mathrm{m}}}{dt} + Q_{\mathrm{m}}, \tag{1}$$

where dM_{m}/dt is the charging mass flow of the standard chamber, which can be calculated by (2). Q_{m} is the heat exchange between the master cavity and the external environment, which has relationship with temperature difference, heat exchange area, and heat transfer coefficient as (3).

$$\frac{dM_{\mathrm{m}}}{dt} = \begin{cases} C_{\mathrm{m}} \rho_{\mathrm{ANR}} P_s \sqrt{\dfrac{T_{\mathrm{ANR}}}{T_{\mathrm{s}}}} \sqrt{1 - \left(\dfrac{P_{\mathrm{m}}/P_{\mathrm{s}} - b_{\mathrm{m}}}{1 - b_{\mathrm{m}}}\right)^2}, & \dfrac{P_m}{P_{\mathrm{s}}} > b_{\mathrm{m}}, \\ C_{\mathrm{m}} \rho_{\mathrm{ANR}} P_{\mathrm{s}} \sqrt{\dfrac{T_{\mathrm{ANR}}}{T_{\mathrm{s}}}}, & \dfrac{P_{\mathrm{m}}}{P_{\mathrm{s}}} \le b_{\mathrm{m}}, \end{cases} \tag{2}$$

$$Q_{\mathrm{m}} = h_{\mathrm{m}} S_{\mathrm{m}} (T_{\mathrm{m}} - T_a). \tag{3}$$

Take expressions (2) and (3) into Equation (1) and get expression (4), there is,

$$\frac{dT_{\mathrm{m}}}{dt} = \frac{R T_{\mathrm{m}}}{C_v P_{\mathrm{m}} V_{\mathrm{m}}} \left[\frac{dM_{\mathrm{m}}}{dt} \left(C_p T_a - C_v T_{\mathrm{m}} \right) + h_{\mathrm{m}} S_h (T_a - T_{\mathrm{m}}) \right]. \tag{4}$$

The gas in the master chamber is regarded as an ideal gas, and the equation of state of the ideal gas is obtained.

$$\frac{dP_{\mathrm{m}}}{dt} = \frac{P_{\mathrm{m}}}{T_{\mathrm{m}}} \frac{dT_{\mathrm{m}}}{dt} + \frac{R T_{\mathrm{m}}}{V_{\mathrm{m}}} \frac{dM_{\mathrm{m}}}{dt}. \tag{5}$$

The above Equations (4) and (5) can describe the changes of pressure and temperature in the master chamber during charging.

For the tested chamber, similar to the above, Equations (6) and (7) can be obtained according to the energy conservation and the ideal gas equation of state. The difference is that there is also mass exchange M_{e} caused by the leakage

of the chamber.

$$\frac{dT_w}{dt} = \frac{RT_w}{C_v P_w V_w}\left[\frac{M_w}{dt}\left(C_p T_a - C_v T_w\right) - RT_w \frac{M_e}{dt} + h_w S_w (T_a - T_w)\right], \tag{6}$$

$$\frac{dP_w}{dt} = \frac{P_w}{T_w}\frac{dT_w}{dt} + \frac{RT_w}{V_w}\left(\frac{M_w}{dt} - \frac{M_e}{dt}\right). \tag{7}$$

Considering that the leakage mass flow is far larger than inflation mass flow, the influence caused by leakage can be ignored in the charging stage, and Equations (6) and (7) can be simplified into the following two equations.

$$\begin{aligned}\frac{dT_w}{dt} &= \frac{RT_w}{C_v P_w V_w}\left[\frac{M_w}{dt}\left(C_p T_a - C_v T_w\right) + h_w S_w (T_a - T_w)\right],\\ \frac{dP_w}{dt} &= \frac{P_w}{T_w}\frac{dT_w}{dt} + \frac{RT_w}{V_w}\left(\frac{M_w}{dt} - \frac{M_e}{dt}\right),\end{aligned} \tag{8}$$

where M_w/dt can be calculated by the formula of

$$\frac{M_w}{dt} = \begin{cases} C_w \rho_{ANR} P_s \sqrt{\dfrac{T_{ANR}}{T_s}} \sqrt{1 - \left(\dfrac{P_w/P_s - b_w}{1 - b_w}\right)^2}, & \dfrac{P_w}{P_s} > b_w, \\ C_w \rho_{ANR} P_s \sqrt{\dfrac{T_{ANR}}{T_s}}, & \dfrac{P_w}{P_s} \le b_w. \end{cases} \tag{9}$$

2.3. Measurement Process Modelling. During the measurement, the air source interrupts the charging to the two chambers, and the two chambers are isolated from each other. At this stage, the master chamber only has heat exchange with the environment, while the chamber to be measured has heat exchange with the environment, and the mass is reduced due to leakage.

For the master chamber, the charging mass flow in the charging state Equations (4) and (5) is to be zero, and the following measurement process state equations can be obtained, as shown in

$$\frac{dT_m}{dt} = \frac{RT_m}{C_v P_m V_m}[h_m S_m (T_a - T_m)], \tag{10}$$

$$\frac{dP_m}{dt} = \frac{P_m}{T_m}\frac{dT_m}{dt}. \tag{11}$$

Similarly, the charging mass flow of the tested volume in the charging state Equations (6) and (7) is to zero, and the following measurement state Equations (12) and (13) are obtained.

$$\frac{dT_w}{dt} = \frac{RT_w}{C_v P_w V_w}\left[-RT_w \frac{M_e}{dt} + h_w S_w (T_a - T_w)\right], \tag{12}$$

$$\frac{dP_w}{dt} = \frac{P_w}{T_w}\frac{dT_w}{dt} - \frac{RT_w}{V_w}\frac{M_e}{dt}. \tag{13}$$

According to Equations (11) and (13), the relationship between differential pressure and leakage can be obtained, as shown in

$$\frac{d\Delta P}{dt} = \frac{dP_w}{dt} - \frac{dP_m}{dt} = \frac{P_w}{T_w}\frac{dT_w}{dt} - \frac{RT_w}{V_w}\frac{M_e}{dt} - \frac{P_m}{T_m}\frac{dT_m}{dt}. \tag{14}$$

In theory, when the equilibrium time is long enough, the differential of the two cavities approaches zero, then the above Equation (14) can be simplified as follows:

$$\frac{d\Delta P}{dt} = -\frac{RT_w}{V_w}\frac{dM_e}{dt}, \tag{15}$$

that is,

$$\frac{dM_e}{dt} = -\frac{V_w d\Delta P}{RT_w dt}. \tag{16}$$

3. Simulation Result

3.1. Simulation Structure. The simulation system gives the input flow and leakage flow and calculates the pressure and temperature of master chamber and tested chamber and then brings it into the leakage formula. Comparing the output value of the leakage formula with the given leakage flow can reflect the effectiveness of the formula.

In the simulation, the charging volume and leakage volume are set, respectively, expressed by step function. The simulation time is 20 seconds. The leakage volume of the tested chamber remains 1 L/min, and the leakage volume of the master chamber is zero. Among them, the *s*-function in MATLAB program of the standard cavity state includes initialization, differential calculation, and output. The charging and leakage are taken as inputs u_1 and u_2, and the pressure and temperature in the air tank are taken as intermediate variable.

The parameters during simultaneous initialization are shown in Table 1. After simulation, the pressure and temperature values of the master chamber and the tested chamber are obtained, and formula (16) is used to calculate the leakage as the simulation result.

3.2. Relationship between Volume and Calculated Leakage. In order to get the relationship between the volume of the master chamber and the leakage detection, the tested volume is given 5 L, copper is used as the heat transfer material, the heat transfer area is set as 0.02 m^2, and the master chambers with different volumes are set as 3 L, 5 L, and 10 L. The heat transfer situation is the same as that of the tested chamber. In the charging and balance stage, the pressure of the two tanks reaches 5 bar, and the temperature reaches 300 K, and then, the leakage signal of 1 L/min is provided. The leakage is calculated according to the simulation framework, and the calculated

Table 1: Parameters of simultaneous initialization.

Parameter	Value	Parameter	Value
Atmospheric temperature	293 K	Atmospheric pressure	1.01 kPa
Gas thermodynamic constant	287 N•m/(kg•K)	Constant volume coefficient	718 J/(kg•K)
Constant pressure coefficient	1005 J/(kg•K)		

data are returned to the inverted MATLAB work area. The results are shown in Figure 2.

In the process of leak detection, the pressure in the two gas tanks is decreasing, but the decreasing amplitude is different. Their difference can reflect the leakage. As shown in Figure 2(a), the pressure difference between different master tanks and the tested tank can be seen. When the volumes of the two gas tanks are the same, the pressure difference increases slowly. When the volume of the master tank is larger, the pressure difference increases sharply at first. After that, the amplitude increases slowly. When the volume of the master tank is smaller, the pressure of the master tank decreases faster than that of tested tank in the initial stage, because the pressure is inversely proportional to the volume according to the ideal gas state equation, and then, the pressure difference between the two gas tanks becomes positive and increases continuously, which is caused by the leakage of tested tank.

In terms of temperature, the temperature difference curves of different master cavities are shown in Figure 2(b). During the leak detection process, the overall trend of the temperature difference in the two gas tanks is increasing, but for the 3 L gas tank, the temperature difference first decreases by nearly 2 K and then increases. For the 3 L gas tank, the temperature difference increases by over 3.7 K and then decreases until the curve coincides with 5 L. It can be inferred that when the volume of the master gas tank is the same as that of the tested tank, the temperature difference increases steadily and slowly. When the volume of the standard gas tank is larger, the temperature difference first increases and then decreases until it reaches the trend of slow increase. When the volume of the standard gas tank is smaller, the temperature difference first decreases and then increases until it reaches the trend of slow increase. The greater the difference in the volume of the gas tank, the more obvious the fluctuation is.

In terms of leakage calculation, the leakage calculation value of 10 L gas tank decreases from more than 9 L/min and slowly increases to 1 L/min after reaching about 25 s. The leakage calculation of 5 L gas tank faster attains about 1 L/min, and the leakage of 3 L gas tank increases from over -9 L/min until it is stable.

3.3. Relationship between Heat Transfer Coefficient and Calculated Leakage. For getting the relationship between the heat transfer coefficient of the master cavity and the leakage detection, the heat transfer material of the master volume chamber with different heat transfer materials is copper, iron, and aluminum, with the volume of 5 L, and the heat transfer area 0.02 m^2, so that the heat transfer coefficient of different heat transfer material will be 401 W/mK, 237 W/mK, and 80 W/mK, respectively. In the charging and balance stage, the pressure of the two air tanks reaches 5 bar, and the temperature reaches 300 K; then, provide the leakage signal of 1 L/min. The leakage is calculated according to the simulation framework, and the calculated data is returned to the working area. The results are shown in Figure 3.

In the process of leak detection, the pressure in the two gas tanks is decreasing, but the decreasing amplitude is different. Their difference can reflect the leakage. As shown in the above Figure 3(a), the pressure difference between different master tanks and the tested tank is shown. When the heat transfer conditions of the two gas tanks are the same, the pressure difference increases slowly. When aluminum is used for heat transfer, the pressure difference increases sharply first, and then, the increasing amplitude slows down. When iron is used for heat transfer, the situation is in the middle.

In terms of temperature, the temperature difference curves of different master cavities are shown in Figure 3(b). During the leakage detection process, the overall trend of the temperature difference in the two gas tanks is rising slowly, but for the copper gas tank, the temperature difference increases stably and slowly. For the aluminum gas tank, the temperature difference increases first and then decreases slowly. When iron is used for heat transfer, the situation is in the middle. It can be seen that the heat transfer material of the gas tank has a severe impact on the temperature difference calculation.

In terms of leakage calculation, the calculated leakage value of aluminum gas tank decreases from 13.91 L/min, the calculated value of copper gas tank stabilizes at about 1 L/min, and the calculated value of iron gas tank decreases from 7.79 L/min. It can be seen that keeping the heat transfer material of the same material as the measured gas tank can effectively shorten the measurement time and ensure the measurement accuracy. Otherwise, choosing materials with close heat transfer coefficient can also effectively shorten the time of leakage calculation.

3.4. Relationship between Heat Transfer Area and Calculated Leakage. For simultaneous interpretation of the relationship between the heat transfer area of the master cavity and the leakage detection, the volume of 5 L is taken as tested tank, and the copper is used as the heat transfer material, and the heat transfer area is 0.02 m^2. The master chamber with different heat transfer area is 0.02 m^2, 0.05 m^2, and 0.1 m^2, and the other cases are the same as the tested cavity. The pressure of the two tanks

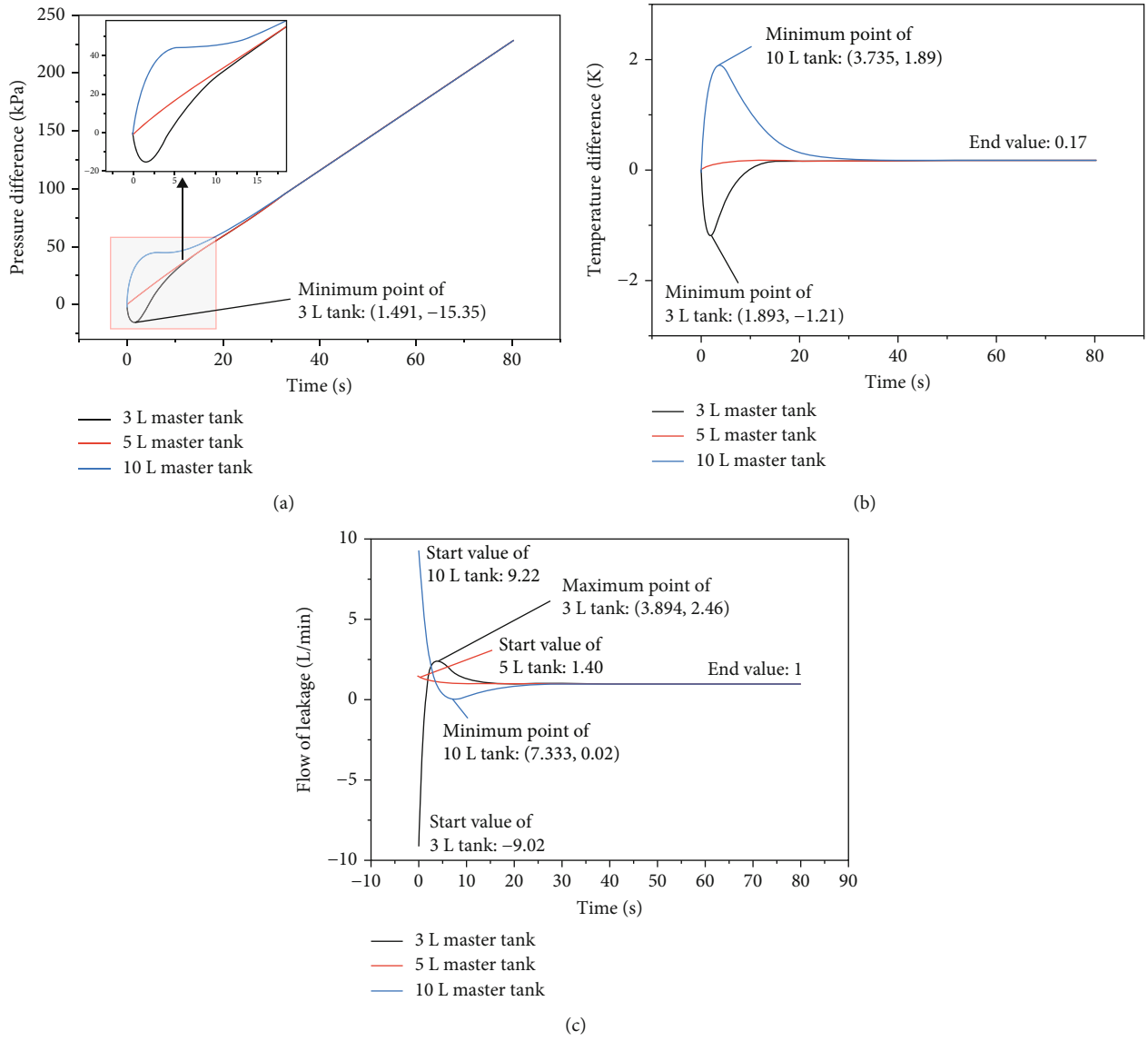

Figure 2: The pressure difference (a), temperature difference (b), and leakage flow (c) relationship of different volume.

can reach 5 bar at the charging and balance stage, and the temperature reaches 300 K. Then, it is provided 1 L/min leakage signal, and the leakage is calculated according to the simulation framework, and the calculated data is returned to the reverse MATLAB work area. The results are shown in Figure 4.

As shown in Figure 4(a), the pressure difference between different master gas tanks and tested tank can be seen. In the initial stage, the larger the heat transfer area, the faster the pressure drop in the master chamber, so the pressure difference is negative. However, with the progress of air leakage, the pressure difference of 0.1 m^2 increases after 1 s, and the final trend is increasing.

In terms of temperature, the temperature difference curves of different standard cavities are shown in Figure 4(b). During the leakage detection process, the overall trend of the temperature difference is rising slowly, but the temperature of the master cavity with large heat transfer area decreases rapidly, resulting in the temperature difference first being negative and then slowly reaching positive.

In terms of leakage calculation, the calculated value of leakage calculation with large heat transfer area increases from lower point due to the influence of low pressure difference and low temperature, and finally, all of them tend to be stable.

3.5. Simulation Results of Ideal Isothermal Cavity. Quasi-isothermal cavity refers to a cavity with good heat transfer. It keeps the temperature unchanged or increases slowly, but it is different from the ideal isothermal environment. Compared with the ideal environment and the real quasi-isothermal cavity, the calculation and simulation of leakage is shown in Figure 5.

The differential pressure of the ideal gas tank keeps increasing continuously, and the increasing trend increases first and then slowly, while the differential pressure of the

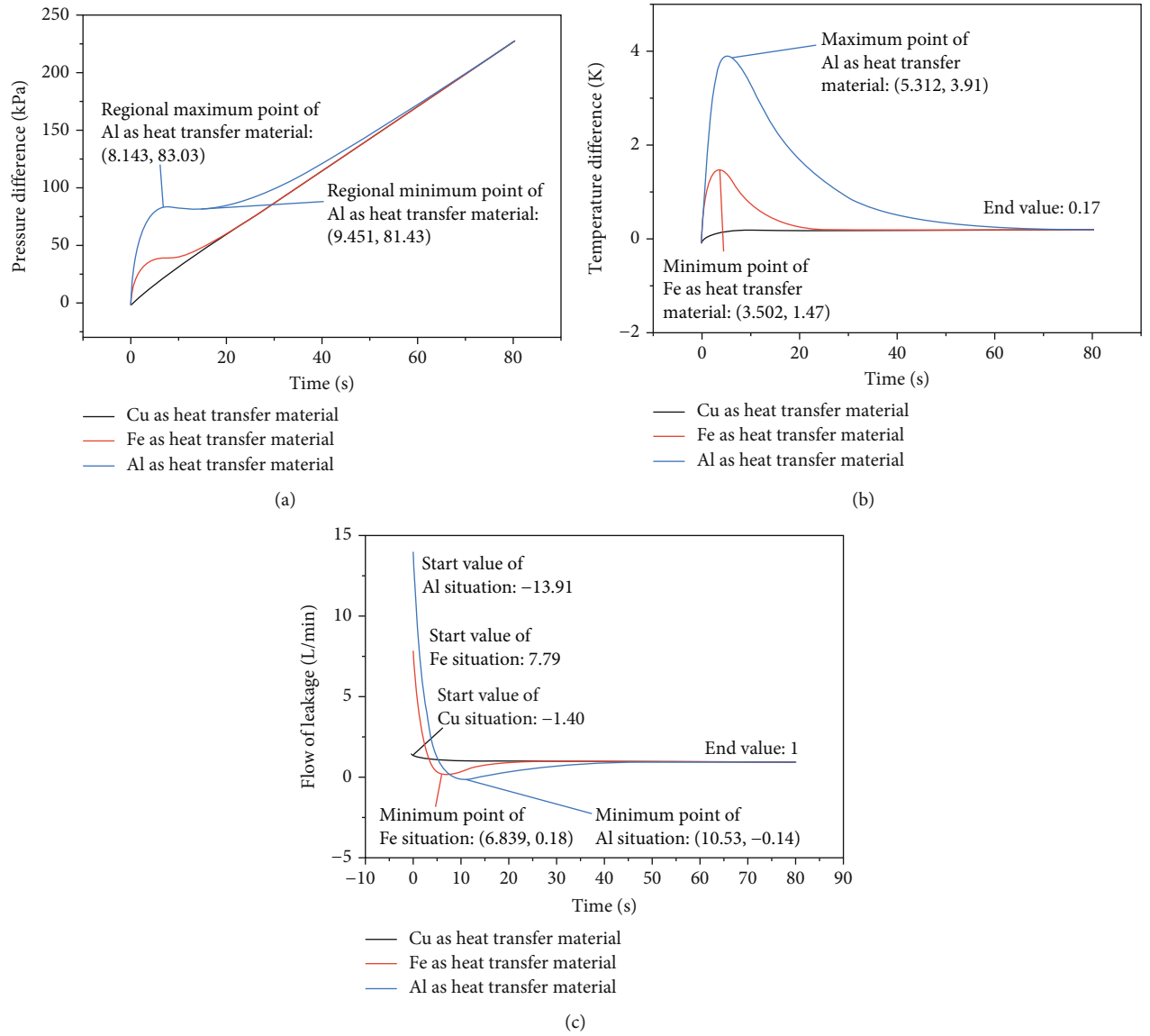

Figure 3: The pressure difference (a), temperature difference (b), and leakage flow (c) relationship of different heat transfer coefficient.

quasi-isothermal gas tank hardly increases in the early stage and begins to increase in about 2 s slowly.

In terms of temperature, the ideal gas tank keeps increasing continuously and increases slowly near 7 K in about 5 s, while the differential pressure of quasi-isothermal gas tank first decreases to 1 L/min and then increases slowly.

In terms of leakage calculation, the calculated value of ideal gas tank decreases from 10 L/min and that of quasi-isothermal gas tank increases from −5 L/min until they coincide.

4. Experiment Result

4.1. Introduction to Experimental Equipment. In the experiment, air compressor, air tank, flow sensor, pressure sensor, temperature sensor, acquisition equipment, and host computer are used, and flow proportional valve is used to provide leakage. Among them, 3 L and 5 L are used for the tested tank, 20 L is used for the master tank, HFT-800 sensor provided by ECOSO company is used for the flow sensor, platinum wire in the range of 0-50°C is used as the thermistor for the temperature sensor, and the resistance value is collected and converted into electric voltage signal. The voltage signal of each sensor is calculated as the actual physical value in the upper computer through the acquisition board USB6001 of National Instruments Company. The proportional valve uses FESTO-MYPE series valve. The valve has a position control valve core, which can convert the analog input signal into the corresponding opening size of the valve output port. The experimental site picture and structure diagram are shown in Figure 6.

During the experiment, the valve is opened between the air tank and the air compressor for charging, then open the valve connecting the two air tanks to balance the pressure in the two air tanks, and then, the connecting valves of the two air tanks are closed. The whole process is recorded by sensors, and the measurement results can be used for leakage calculation.

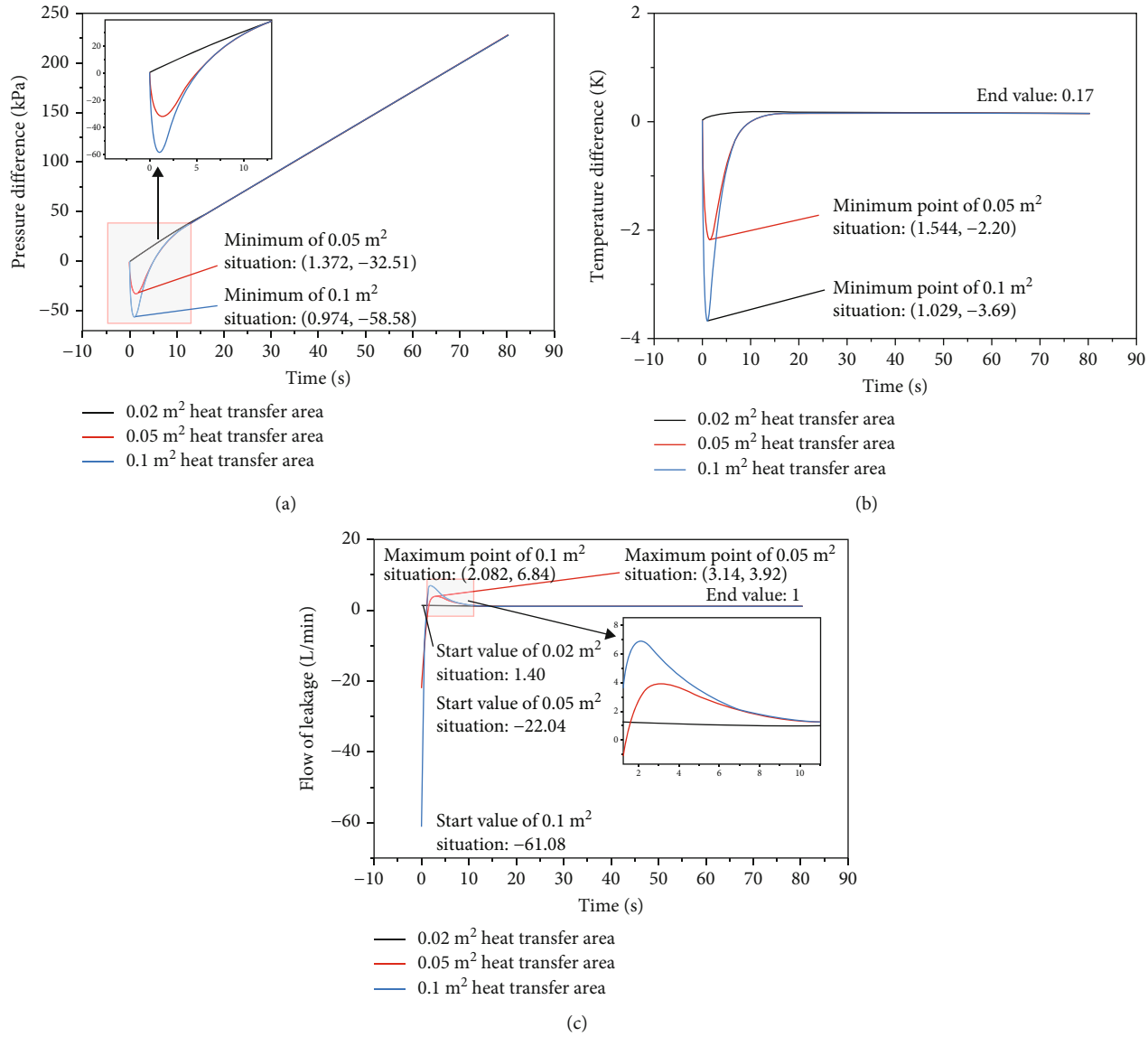

Figure 4: The pressure difference (a), temperature difference (b), and leakage flow (c) relationship of different heat transfer area.

4.2. Experimental Result of 3 L Tank. The pressure of the master air tank and tested tank with 3 L during the charging process is same, but they start different at measurement. During the measurement process, the pressure of the master tank gradually decreases because the cooling of heat transfer material in tank, reducing the pressure in the air tank, while that of the tested tank decreased because of air leakage and cooling.

Figure 7(a) shows the pressure changes in the two chambers. The pressure is synchronous and relatively stable in the charging stage. However, in the measurement stage, due to the existence of leakage and temperature exchange, the pressure of the chamber to be measured continues to drop, from 0.44 MPa to 0.12 MPa in the measurement period from 185.3 s to 505 s, while the master chamber is only affected by temperature exchange. Therefore, the pressure of the standard chamber decreases slowly and decreases to 0.41 MPa in the measurement period. In order to obtain the pressure difference measured discretely in the experiment, according to Equations (11) and (13), it is noted that the differential of the pressure drop and the pressure drop approximately satisfy the subtraction of two exponential functions. Since the measured discrete value cannot calculate the continuous differential quantity, the pressure difference is fitted. The fitting result is as shown in Equation (17). The fitting effect R-square attains 0.9999, which indicates that the fitting effect is good.

$$\frac{d\Delta p_{3L}}{dt} = 0.347 \times \exp\left(-0.00713 \times t\right) - 0.347 \times \exp\left(-0.00029 \times t\right). \tag{17}$$

The derivative of the fitting curve is obtained and substituted into the results of (16). The comparison diagram between the flow value finally obtained and the collected value of the smoothed flowmeter is shown in Figure 7(b). During the measurement process, the minimum difference reaches 0.0037 mL/min, the minimum position occurs at

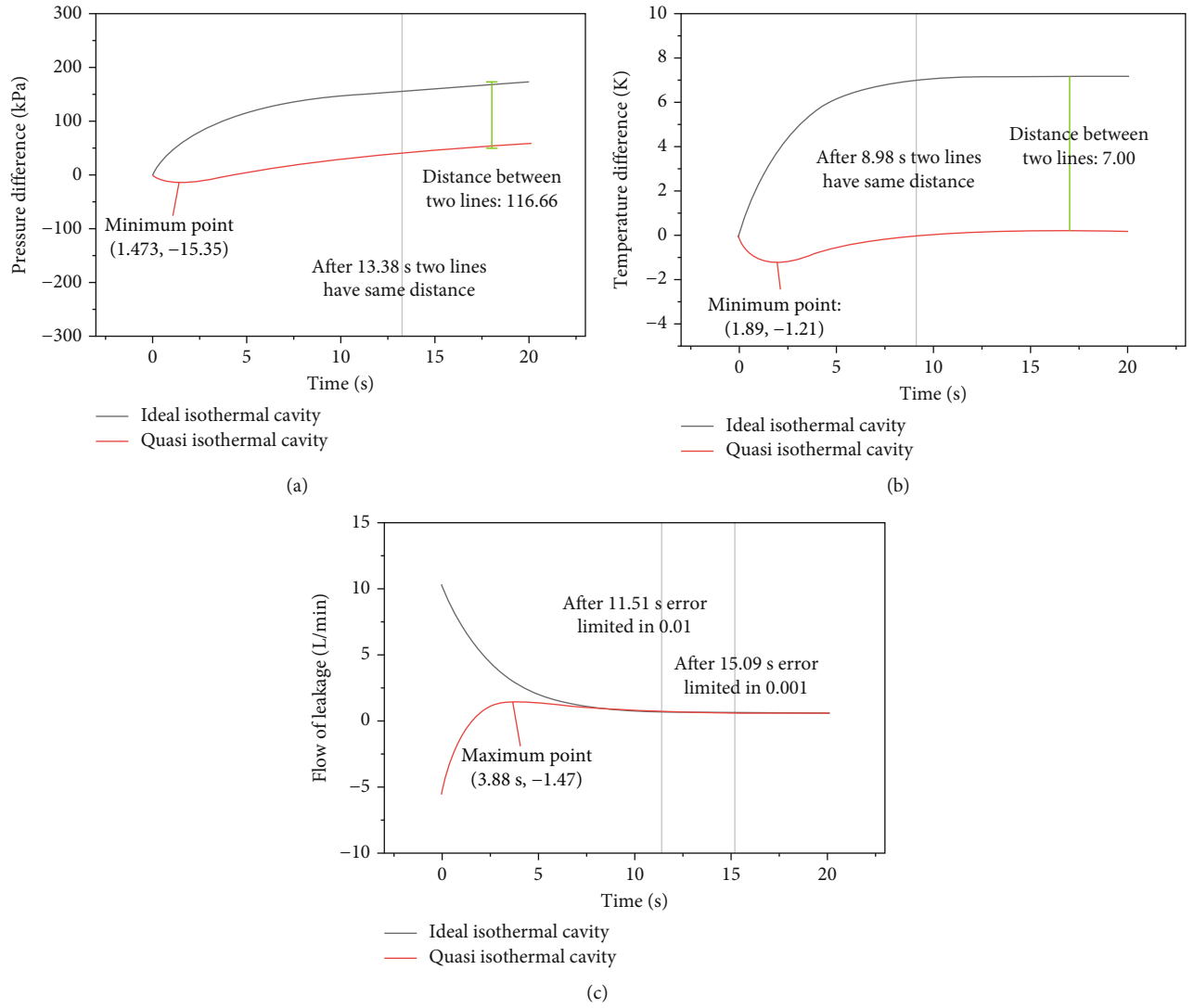

Figure 5: The pressure difference (a), temperature difference (b), and leakage flow (c) relationship of different type of isothermal cavity.

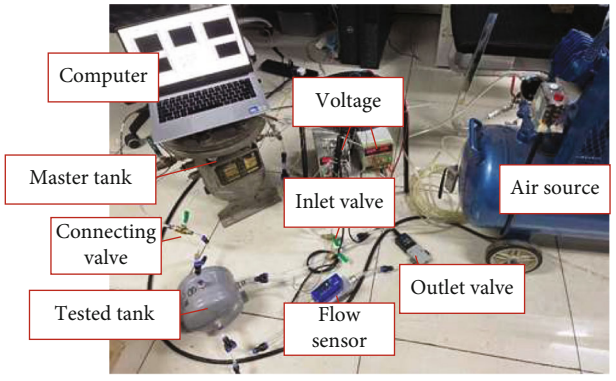

Figure 6: Experimental site picture.

the time of 196.3 s, and the maximum difference reaches 39 mL/min at the time of 345.3 s. The detection deviation is 14.4%. The reason for larger deviation in the later stage of measurement is due to the much decrease of pressure of tested chamber, which is close to the atmospheric pressure, resulting in a decrease in measurement accuracy and a large calculation error. This also shows that the method has higher accuracy under high pressure, and the accuracy will be reduced in the case of excessive leakage. Moreover, the pressure sensor has high measurement accuracy and high speed, which overcomes the problems of low accuracy and poor efficiency of traditional measurement method.

4.3. Experimental Result of 5 L Tank. The trend of pressure of the master air tank and tested tank during charging and measurement is consistent with that of the 3 L tested tank. Figure 8(a) shows the pressure changes in the two chambers. During the charging process, the pressure values of the two are kept synchronized until they reach 0.49 MPa. Then, the difference of two tanks increases due to the cooling effect of the master tank and the cooling and leakage of the tested tank. The pressure in the tested tank is reduced to 0.14 MPa, while that in the master tank is 0.48 MPa. The measurements were started at 183 s and 587 s, and the results were fitted as

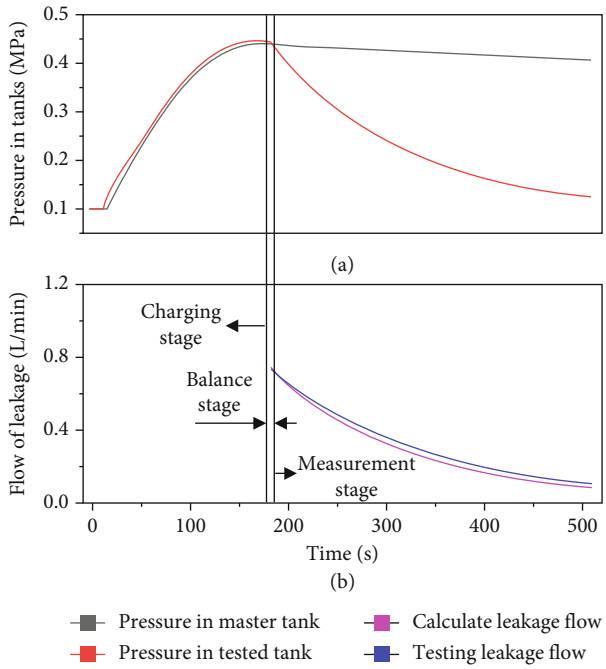

Figure 7: Pressure and calculated leakage flow rate of 3 L tested tank.

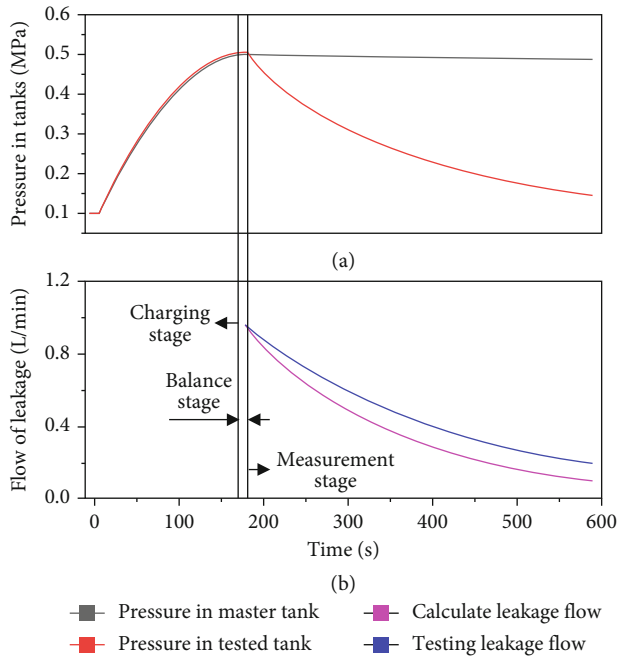

Figure 8: Pressure and calculated leakage flow rate of 5 L tested tank.

shown in

$$\frac{d\Delta p_{5L}}{dt} = 0.345 \times \exp\left(-0.005637 \times t\right) - 0.345 \times \exp\left(-0.00021 \times t\right). \tag{18}$$

It is shown in Figure 8(b) by calculating the 5 L tank leakage value and comparing the corresponding flow detection value. The minimum error is 69.68 mL/min in 183 s, and the maximum error is 412.4 mL/min in 386.7 s, with a deviation rate of 28.3%. Similar to the results measured in the 3 L tank experiment, this method maintains superior applicability in measuring the leakage of the 5 L tank.

Compared with the two experiments, the pressure increase and temperature increase in the 5 L tank are more intense, which verified the simulation of relationship between volume and calculated leakage. The calculated value and the detected value are similar within the allowable error range. And the error is mainly caused by the measurement error of the pressure sensors.

5. Discussion

In the process of simulation and experiment, the precautions for differential pressure test could be concluded.

A basic condition of symmetrical differential pressure detection is that the temperature of the two chambers should be equal. However, due to the change of gas flow and volume during charging, the gas temperature in the measurement process will change, leading to the change of pressure. In this way, the measurement cannot be carried out until the gas entering the system reaches complete balance. The balance time will affect the measurement efficiency. Therefore, the shape, size, material, and wall thickness of the sample volume cavity should be the same as that of the measured workpiece. At the same time, the same interface sealing conditions should be used to make the energy exchange between the gas on both sides of the sensor the same, so as to offset the influence of temperature on the measurement process.

Before the experiment, the system leakage detection should be carried out. The master chamber and the tested chamber should be charging at the same time. After stopping the inflation, keep the pressure for a period to see whether the vacuum degree of the system decreases. If necessary, the connectors should be sealed with sealant. Due to the detection error caused by the pressure change of the test system, the standard and test material must be fully considered when developing the leakage detection equipment.

After the vacuum pumping is completed and the vacuum source is cut off, the vacuum degree in the master chamber and the tested chamber may not be equal due to the length of the pipeline, the inner diameter of the connecting pipe, and the pore size of the liquid supply chamber. Therefore, it is necessary to cut off the path between the comparison source and the measured workpiece after balancing for several seconds. This path is controlled by the valve, but there would be pressure impact when the valve is closed. Therefore, it should be stable for several seconds before starting the test.

6. Conclusions

The leakage of compressed air is mainly caused by the tiny pores of pneumatic components. However, the current method cannot effectively detect the leakage in the harsh

environment and the complex structure of the measured cavity situation. The existing differential pressure detection method is improved in this paper. By introducing the non-leakage master cavity, the pressure difference between the reference cavity and the measured cavity with leakage is obtained, and combining with temperature, the rapid extraction of leakage is realized, and the accurate measurement of leakage of the cavity is obtained.

In the simulation, the influences of the inherent parameters of the master cavity on the pressure difference, temperature difference, and leakage calculation of the master and tested cavities are analyzed. Finally, the tested cavities are set to 3 L and 5 L tanks, respectively, to analyze the accuracy of this model in the experiment. Experimental process maintains same leakage opening of tanks. In the experiment, the maximum experimental error of 3 L tank is 39 mL/min with 14.4% detection error, while the maximum experimental error of 5 L tank is 412.4 mL/min with 28.3% detection error. It is basically consistent with the simulation results and has great improvement compared with previous leak detection methods. Experiments also show that the leakage can be measured accurately in a fast time.

In the future stage, a series of improvements should be made. Not only the temperature compensation method should be used to reduce the measurement time but also a variety of leakage methods and leakage quantities should be selected to make this study more universal. After continuous improvement, this leakage test method would be of great significance to improve the inspection and testing level and manufacturing quality of pneumatic components and promote the development of pneumatic industry.

Nomenclature

p_s: Gas source pressure
p_m: Master chamber pressure
p_w: Tested chamber pressure
p_s: Environmental pressure
V_m: Master cavity volume
T_s: Gas source temperature
T_m: Master chamber temperature
T_w: Tested chamber temperature
T_a: Environmental temperature
V_w: Tested cavity volume
M_m: Master cavity mass increment
M_e: Leakage quality of tested chamber
M_w: Tested cavity heat exchange
Q_m: Master cavity heat exchange
Q_w: Tested cavity heat exchange
C_v: Constant volume heat capacity
C_p: Constant pressure heat capacity
C_m: Master cavity sonic conductance
ρ_{ANR}: Air density under standard conditions
T_{ANR}: Standard condition temperature
b_m: Master cavity critical pressure ratio
h_m: Heat dissipation coefficient of master cavity
S_m: Heat dissipation area of master cavity
C_w: Tested cavity sonic conductance
b_w: Tested cavity critical pressure ratio
h_w: Heat dissipation coefficient of tested cavity
S_w: Heat dissipation area of tested cavity
Δp_{3L}: Pressure difference between master tank and 3 L tested tank (MPa)
Δp_{5L}: Pressure difference between master tank and 5 L tested tank (MPa)
t: Time value of measurement process (s).

Data Availability

The data used to support the findings of this study are available from the corresponding author upon request.

Conflicts of Interest

The authors declare that there is no conflict of interest regarding the publication of this paper.

Acknowledgments

This work was supported by the Youth Fund of National Natural Science Foundation of China (grant no. 52105044), National Key R&D Program of China (grant no. 2019YFC0121702), and National Key R&D Program of China (grant no. 2019YFC0121703).

References

[1] Y. Shirato, W. Ohnishi, H. Fujimoto, T. Koseki, and Y. Hori, "Controller design of mass flow rate loop for high-precision pneumatic actuator," in *2020 IEEE 16th International Workshop on Advanced Motion Control (AMC)*, Kristiansand, Norway, 2020.

[2] A. Sather, C. Arakaki, C. Ratnayake, and D. Di Ruscio, "Prediction of mass flow rate in pneumatic conveying using a system identification modeling approach," *Particulate Science & Technology*, vol. 27, no. 4, pp. 314–326, 2009.

[3] Y. Zheng and L. Qiang, "Review of certain key issues in indirect measurements of the mass flow rate of solids in pneumatic conveying pipelines," *Measurement*, vol. 43, no. 6, pp. 727–734, 2010.

[4] C. Arakaki, C. Ratnayake, and M. Halstensen, "Online prediction of mass flow rate of solids in dilute phase pneumatic conveying systems using multivariate calibration," *Powder Technology*, vol. 195, no. 2, pp. 113–118, 2009.

[5] M. Zeidouni, M. Pooladi-Darvish, and D. W. Keith, "Leakage detection and characterization through pressure monitoring," *Energy Procedia*, vol. 4, pp. 3534–3541, 2011.

[6] X. Liu, J. Liu, and S. Li, "Parameter modification model of fluid flow rate for a pneumatically-actuated PDMS membrane microvalve," in *2015 International Conference on Fluid Power and Mechatronics (FPM)*, Harbin, China, 2015.

[7] S. Wei, R. Yan, L. Sun et al., "Study of the space station on-orbit leak detection based on the differential pressure gas sensor," in *2013 IEEE International Conference on Green Computing and Communications and IEEE Internet of Things and IEEE Cyber, Physical and Social Computing*, Beijing, China, 2013.

[8] S. R. Ravula, S. C. Narasimman, L. Wang, and A. Ukil, "Experimental validation of leak and water-ingression detection in

low-pressure gas pipeline using pressure and flow measurements," *IEEE Sensors Journal*, vol. 17, no. 20, pp. 6734–6742, 2017.

[9] C. C. Daniels, M. J. Braun, H. A. Oravec, J. L. Mather, and S. C. Taylor, "Leak rate quantification method for gas pressure seals with controlled pressure differential," *Journal of Spacecraft and Rockets*, vol. 54, p. 6, 2013.

[10] H. H. Xiao, T. Wang, and W. Fan, "Study on leaking detecting by ultrasonic testing system with leak hole estimation," *Applied Mechanics and Materials*, vol. 235, pp. 204–209, 2012.

[11] G. R. Piazzetta, R. Flesch, and A. Pacheco, "Leak detection in pressure vessels using ultrasonic techniques," in *SME 2017 Pressure Vessels and Piping Conference. Volume 5: High-Pressure Technology; ASME Nondestructive Evaluation, Diagnosis and Prognosis Division (NDPD); SPC Track for Senate*, Waikoloa, Hawaii, USA, 2017.

[12] T. Wang, X. Wang, and M. Hong, "Gas leak location detection based on data fusion with time difference of arrival and energy decay using an ultrasonic sensor array," *Sensors*, vol. 18, no. 9, article 2985, 2018.

[13] T. Wang, X. Wang, B. Wang, and W. Fan, "Gas leak location method based on annular ultrasonic sensor array," in *2018 IEEE International Instrumentation and Measurement Technology Conference (I2MTC)*, Houston, TX, USA, 2018.

[14] D. Wang, F. Zhao, and T. Wang, "The ultrasonic characteristics study of weak gas leakage," in *2015 International Conference on Fluid Power and Mechatronics (FPM)*, Harbin, China, 2015.

[15] J. Wang, L. Zhao, T. Liu, Z. Li, T. Sun, and K. T. V. Grattan, "Novel negative pressure wave-based pipeline leak detection system using fiber Bragg grating-based pressure sensors," *Journal of Lightwave Technology*, vol. 35, no. 16, pp. 3366–3373, 2017.

[16] M. A. Baballe and M. I. Bello, "Gas leakage detection system with alarming system," *Review of Computer Engineering Research*, vol. 9, no. 1, pp. 30–43, 2022.

[17] Q. Tan, X. Mu, M. Fu et al., "A new sensor fault diagnosis method for gas leakage monitoring based on the naive Bayes and probabilistic neural network classifier," *Measurement*, vol. 194, article 111037, 2022.

[18] Z. Chi, J. Jiang, X. Diao et al., "Novel leakage detection method by improved adaptive filtering and pattern recognition based on acoustic waves," *International Journal of Pattern Recognition and Artificial Intelligence*, vol. 36, no. 2, 2022.

[19] M. Jahanian, A. Ramezani, A. Moarefianpour, and M. Aliari Shouredeli, "Gas pipeline leakage detection in the presence of parameter uncertainty using robust extended Kalman filter," *Transactions of the Institute of Measurement and Control*, vol. 43, no. 9, pp. 2044–2057, 2021.

[20] R. Doshmanziari, H. Khaloozadeh, and A. Nikoofard, "Gas pipeline leakage detection based on sensor fusion under model-based fault detection framework," *Journal of Petroleum Science and Engineering*, vol. 184, article 106581, 2020.

[21] L. Zhao, T. Wang, P. Shi, and M. Wang, "A novel adaptive leak diagnosis and localization method for infrared image," *International Journal of Innovative Computing Information & Control*, vol. 8, no. 5B, pp. 3553–3563, 2012.